SCHOOL OF ELECTRICAL ENGINEERING, UNIVERSITY OF THE WITSWATERSRAND

ELEN3017 - Electrical Engineering Design

Lecturer: James Braid

Optimisation of a Solar PV installation

6 March 2018

Tyson Cross 1239448

Abstract

This report details the analysis and design of a fixed-angle 1.2kW solar photovoltaic cell array for an off-grid connected rural community centre to be located in Graaf-Reinet, South Africa. The optimal fixed panel tilt angle is calculated with reference to the sun's annual path with a weighted-average method. A simplified, practical single-diode equivalent circuit from existing literature, based on parameters available on the datasheet for the PV array, is used to simulate the behaviour of a PV cell in relationship to solar irradiance and air temperature. The results of a model with a fixed resistance load of $10\,\Omega$and one using a MPPT system are compared and discussed with regards to power harvesting, cost and maintenance.

1 INTRODUCTION

The sun continually emits vast amounts of energy, some of which which strikes the surface of the earth as the planet revolves around it. Photovoltaic cell technology can capture a portion of this electromagnetic spectrum, transforming energy into electricity which can be used to power devices to perform useful work. However, the irregular tilt of the earth along its longitudinal axis, and the slightly elliptical shape of the earth's annual orbit result in daily and seasonal variations in the available energy at any given point upon the surface of the globe. Self-occlusion from the rotational of the earth itself results in a day-night cycle, further restricting the available hours of sunlight. The regular movement and path of the sun through the sky is highly predictable[1], and the subject of much study and analysis[2], [3], [4], [5], [1].

The complex pattern of atmospheric air-mass and optical interaction in response to the cyclical heating and cooling of the planet produces weather causes several complex and less-predictable factors. Cloud cover causes shadowing of the PV panels, reducing their efficiency. Lensing effects from the atmosphere results in scattering, attenuation through absorption and bending of the light-rays, reducing the total terrestrial solar irradiance to an approximate value of $1\,\mathrm{kW\,m^{-2}}$ at noon. This report does not consider the atmospheric effects or the contribution of diffuse horizontal irradiance (DHI), and regards the available direct normal solar insolation (DNI) from the available site measurements of a year's data collected by the Southern African Universities Radiometric Network (SAURAN)[6], and calculations from analytic literature regarding the sun's path.

2 SOLAR VECTOR

From a perspective on the earth's surface, the angle of the sun's elevation from the horizon to the surface normal is the *altitude* or *elevation* angle α. Its compliment from the surface normal at $0°$, down towards the horizon line at $90°$, is called the *zenith* angle ζ. Variance in the sun's apparent path from east to west is the *azimuth* angle γ. Due to the tilt of the earth, and the elliptical motion around the sun, an additional relative path described by the *declination* angle δ must be considered. There is an abundance of theory and data to calculate the relative position of the sun using these angles for any time and from any location [7]. The solar equinoctes at the site are 21 December for the summer equinox and the winter extreme is on 21 June. The highest and lowest peaks of available sunlight occur at noon on these days. The site solstices occur on the 21 March and 21 September and the relative motion of the sun for these days can be seen in Figure A1 and A2. The variance in zenith angle at different times of the day throughout the year causes large variation in the amount of DNI. With the assumption that the collector surface is a horizontal plane pointing upwards in a flat and open area without shading or reflection, the DHI can be considered negligible, providing a simple formula of total irradiance (or solar intensity *I*) in equation 1:

$$GHI = DNI \times cos(\zeta) \tag{1}$$

The available direct beam energy is maximal if the zenith is directly overhead at $0°$. The annual solar zenith angles for various times of day at the site can be seen in Figure A3.

3 SITE SOLAR INSOLATION

The site for the project is located in Graaf-Reinet at a location shown in Table I. SAURAN has detailed measurements for the location, including the GHI, DHI, DNI and variance in air temperature, at various resolutions (daily, hourly and every ten minutes.)

TABLE I: Site Location

Latitude	Longitude	Elevation
-32.48547	24.58582	660m

3.1 Data and measurements

The SAURAN data was only available for limited period of time, covering full calender years for 2014 and 2015. The data for 2014 was chosen for the calculations, as the solar irradiance measured for the summer and winter equinoctes was largely unoccluded compared to 2015, as seen in Figure A6. Summing the total irradiance measurements over a day is the equivalent of the rectangular area of the height of the noon peak irradiance and the width of useful sun-hours. Taking the average of the equinoctial peaks and hourly widths gives a useful approximation of the total average daily irradiance over the year shown in Table III.

The annual data for 2014 has a gap, where lighting struck the measurement equipment in April 2017. However, using additional data from [7] allowed a formulation of an estimate model. This solar vector equations result in a matching set of curves over this missing period, shown in Figure A7. Note the

disparity between the theoretical model's peak insolation and the quantitative data, particularly during the winter period.

The air temperature during operations of the PV modules must be taken into consideration. There is a large range of noisy annual data shown in Figure A8, with a mean temperature of $18.8\,^{\circ}\mathrm{C}$. The range represented in this data includes the low temperatures at night during winter when the sun is not visible. For the PV cell simulation, only peak values of temperature at noon are used. Some representative values are shown in Table IV.

4 PV Module specifications

The PV array is made up of four TSM-PA14 modules, each with a rated $300\,\mathrm{W}$ max power output at 15.5% efficiency η according to the manufacturer datasheet[8]. Each module has a surface area, specified as $1956\,\mathrm{mm}$ x $941\,\mathrm{mm}$. Together the four panels have a total surface area of $7.36\,\mathrm{m}^2$ and maximum power output of $1.2\,\mathrm{kW}$. With these basic measurements, we can roughly calculate the available daily and annual limit of available energy to the array pointing at the sun, ignoring the reduction from a tilted surface, cloud occlusion and temperature for now.

$$E_{max} = \eta GHI \times A_{pv} \approx 4.4\,\mathrm{kW} \text{ on averaged day} \qquad (2)$$

This approximation does not consider a fixed tilt, any percentage of occlusion or the affect of air temperature on PV cell performance.

5 Tilt and orientation angle determination

The initial project requirement was to determine the optimal angle of the fixed tilt angle β for the PV array, measured as an incident angle from horizontal ($0°$) to the surface normal ($90°$). Optimal β changes each moment of each day throughout the year, with the angle ideally being equal to the sun's zenith angle ζ. The optimal orientation is directly north, the annual average position of the sun's azimuth (see Figure A2.) A graph of the tilt angle β set to the sun's zenith angle at every moment, with an azimuth orientation of $0°$ produces the graph shown in Figure A4. The mean of the annual angle is roughly equal to the latitude of the location, a commonly used rule-of-thumb in PV installations. However, using the weighting method outlined in [9] a slightly more optimal angle can be found. The intensity *I* of insolation striking the collector can be described by equation 3

$$I = I_{incident} sin(\alpha + \beta) \qquad (3)$$

$$\textit{where } \alpha = 90 - \zeta$$

Table V shows the calculated tile angles. As Figure A5 shows, the weighted tilt angle results in slightly higher overall performance, although collection during the winter months is lower than the normal mean.

5.1 Weighting methodology

The weighting methodology outlined in [9] is described in equation I: The weighting results in a very small improvement in overall collection over a year with only a difference of $38\,\mathrm{kW\,h\,m^{-2}}$ in annual collection. Larger surface area would make a bigger impact on optimisation. This weighted value of β is chosen for the optimal tilt value of the array.

6 Mathematical model of a PV cell

A PV cell simulation was programmed in MATLAB, from datasheet parameters, using the method described in [10], [11]. This simplified model reduces the commonly used practical single-diode circuit model (see Figure A12 to a reduced computational form that avoids an iterative analysis, excluding several dissipative factors with the assumptions $R_s \to \inf$ and $R_{sh} \approx 0$. Equation 4 shows the non-simplified model, which contains several other unknown quantities (n, I_o and I_{ph}) that the manufacturer datasheet does not provide. Implementing the full model requires measuring the PV under use, and so the chosen mathematical model is an appropriate choice due to the project limitations. The module configuration is connected in series, and resistive losses from wiring and heat losses are neglected. The temperature coefficients from the datasheet are incorporated in the model.

$$I = I_{ph} - I_o\big(e^{-\frac{q(V+I\cdot R_s)}{nKT_c}} - 1\big) - \frac{V + I \cdot R_s}{R_{sh}} \qquad (4)$$

The reduced form of the simplified equations were implemented in MATLAB (see Code Listing 1) according to the process in [10]. The relevant parameters were entered from the datasheet, and the resulting cell current I_{cell} was calculated with the ten-minute site measurements for radiance (with the chosen optimal tilt value 28.92° and associated air temperature as input parameters.

6.1 MATLAB Simulation

Two possible theoretical operating situations are already established: the peak extremes of summer and winter without any occlusion at noon. Two more scenarios were introduced, again a summer and winter noon but now with some occlusion from common environmental factors. These scenarios are modelled as a coefficient set at 80%, representing weather and other losses to available energy for the system. These four values, along with the temperatures associated with these conditions are input into the MATLAB simulation. The resulting IV and PV curves are shown in Figures A9 and A10 respectively.

7 Simulation parameters

The battery, inverter and amortisation concerns were not discussed in this project. Resistive losses from wiring, electronics, load mismatches and other environmental factors were excluded from the optimisation process. The primary parameters are the air temperature, tilt angle, irradiance intensity and the value of a fixed resistive load required to produce the maximum achievable power from the simulated system.

7.1 Optimal load

To find the optimal resistance, an assumption was made that the MPP at the most amount of sunlight would be the optimal configuration. A loop that evaluated and identified the maximum power point on all IV curves resulting from the input irradiance values (and associated air temperatures) was written in MATLAB. This loop identifies the largest MPP, and then calculates the straight line through the origin and the largest MPP. The value of the optimal resistance is then taken as the inverse of the slope of this line, according to Ohm's law $I/V = R^{-1}$ The remaining voltage and current values for this load value are calculated from the graphical intercept with the straight line passing through the other IV

curves. It is important to note that these lower intercepts are non-optimal, and result in lower power output. Some results are shown in Table VII.

7.2 Maximum power-point tracking

The second scenario that with a maximum power point tracking system with 90% efficiency, maintaining a constant $10\,\Omega$ resistive load at all input incident irradiances striking the tilted PV cell at the summer and winter equinoctes at noon. A graphical analysis was performed on the resulting IV curves, measuring the intercepts of the straight line representing the inverse slope of the resistance, .The intercepts are shown on Figure A9, and listed in TableVI. The intercepts shown in A9 are still not at the MPP for most of the chosen operating scenarios, but the overall sum of the individual power points performs well when available insulation is not at the maximum. A summary of the calculated values are shown in Table VI.

8 Comparison of solutions results

TABLE II: Total harvested energy results

	Day	Day (Occluded)	Year	Year (Occluded)
Ideal	3.93	3.14	1434.77	1147.82
MPPT	2.62	1.91	952.32	698.36
Optimal	3.31	1.66	1207.95	605.68

The maximum theoretical harvested energy, calculated by an idealised solution that matched the MPP of all input irradiances, was established as the simulation limit, to compare the efficiency of the two resistive loads. The results are compared in Table II, where all values given are in [kWhr]. When considering only ideal, sunny weather across, across the average received peak irradiance variation for the year, the optimal solution out-performs the MPPT, harvesting 84% of the maximum power, where the MPPT solution only converts 67% of the maximum achievable power. When accounting for an amount of occlusion, and a maximal theoretical amount of power generated was reduced to 3.14 kWhr/day, and the MPPT solution is better at harvesting energy than the $4.77\,\Omega$ "optimal" solution, by a small amount, around $250\,\mathrm{W}$.

In the annual totals, when considering perfect weather and a tilt angle β set to 28.92°, oriented with the four module panels facing North, a $4.77\,\Omega$ load is predicted to achieve $1207.95\,\mathrm{kW\,h}$, which captures 84% of the maximum power. By contrast, an 90% efficient MPPT system maintaining a fixed load of $10\,\Omega$, was predicted to only managed to harvest 66% of this ideal MPPT system with varying resistance. However, when considering a more realistic situation, with 20% solar occlusion across the year, the "optimal" solution is outperformed by the fixed-load MPPT system. The maximum amount of energy harvested into power by the proposed "optimal" solution is $605.68\,\mathrm{kW\,h}$, 52% of the simulated maximum. The MMPT solution outperforms the $4.77\,\Omega$ "optimal" resistive load, capturing 60% of the maximum power.

9 MPPT cost vs additional PV cells

The cost of power electronics for MPPT systems is discussed in [12], and the cost to performance ratios of various MPPT systems are discussed. Cost, increased complexity and added inefficiencies at low power are concerns when implementing MTTP. Systems such as Constant Voltage, or Open (Circuit) Voltage models are much more affordable expensive than complex solutions such as InCond or ‘P and O ’ solutions which involved more responsive but expensive sensors. The efficiency of the cheaper solutions is typically around 60-75%[12]. The simulated performance presented in this report concludes that the performance of the MPPT is not sufficiently high enough to justify the increased complexity involved with power electronics, particularly in remote rural areas. Increasing the number of modules is a linear cost to benefit ratio, with more afforable components, a linear degradation model over many years and robust construction for a remote environment.

10 Recommendations

In the solution design, the assumption was made that the optimal resistive load occurred when the system was operating in full sunlight on a summers day. The optimisation process would benefit from the introduction of an iterative method, to more rigorously investigate this assumption over more values. As the results show, the MPPT system had better performance and energy harvesting for scenarios where there was greater occlusion and lower total insolation. Additionally, the emphasis on the unoccluded summer noon results in very poor performance during winter when sunlight hours are less, and there is less total insolation. The design specification was to design a system for maximal harvesting of energy, but the resulting design has left the community centres in danger of having insufficient power to operate at all times of the year. Optimising the system for the lowest operating situation, during June, with a suitable tilt angle would result in a more stable and predictable power generation during occluded days as well, at the cost of lower average total power at any given point in time.

11 Conclusion

The total insolation striking the surface at the site location was measured and discussed, along with the solar vectors and related angles that are used to measure and predict the sun’s location in the sky. A tilt angle was found through a weighted mean that maximised solar irradiance collection. A simplified mathematical model of a PV cell was developed in Matlab, and used to simulate the current through the modules in series as a function of irradiance, temperature, an voltage. Results were found for two simulations, the MPPT maintaining a fixed load and an optimal fixed resistance. The results were compared, and the optimal resistance was found to only perform better under sunny conditions, with degraded performance under occluded conditions. The maximum harvested energy for this system over a full year under sunny conditions was found to be $1207.95\,\mathrm{kW\,h}$ with a fixed load of $4.77\,\Omega$, and a tilt angle of 28.92°, facing north. The costs and complexity of adding a MPPT system were briefly discussed, with the conclusion that the most cost effective way and appropriate way to scale up the maximum power of the system would be to add more PV modules.

REFERENCES

[1] J. Duffie, "Solar engineering of thermal processes[electronic resource]," *Access mode: http://www. magsoft. com. pl/˜ herbatniczek/naslon/files/Solar_Engineering_of_Thermal_Processes. pdf*.

[2] A. Al-Khazzar, "A comprehensive solar angles simulation and calculation using matlab," vol. 6, pp. 367–376, 06 2015.

[3] M. Miller, "Maximum power from a solar panel," *Undergraduate Journal of Mathematical Modeling: One+ Two*, vol. 3, no. 1, p. 22, 2010.

[4] Q. Zhao, P. Wang, and L. Goel, "Optimal pv panel tilt angle based on solar radiation prediction," in *Probabilistic Methods Applied to Power Systems (PMAPS), 2010 IEEE 11th International Conference on*. IEEE, 2010, pp. 425–430.

[5] A. Chandrakar and Y. Tiwari, "Optimization of solar power by varying tilt angle/slope 1," 2013.

[6] Centre for Renewable and Sustainable Energy Studies (CRSES), "The Southern African Universities Radiometric Network," http://www.sauran.net.

[7] SunEarthTools.com, "Sun Earth Tools Sun Position finder," https://www.sunearthtools.com/dp/tools/pos_sun.php.

[8] TrinaSolar, "TSM-300 Datasheet," Datasheet.

[9] S. K. Singh, U. A. Jain, and G. Edison, "Matlab/simulink model for optimization of tilt angle of solar panel using weighted average method vit university," *IOSR J. Mech. Civ. Eng.(IOSR-JMCE)*, vol. 11, no. 5, pp. 27–32, 2014.

[10] S. Vergura, "A complete and simplified datasheet-based model of pv cells in variable environmental conditions for circuit simulation," *Energies*, vol. 9, no. 5, p. 326, 2016.

[11] L. Cristaldi, M. Faifer, M. Rossi, and S. Toscani, "A simplified model of photovoltaic panel," in *Instrumentation and Measurement Technology Conference (I2MTC), 2012 IEEE International*. IEEE, 2012, pp. 431–436.

[12] O. Ezinwannea, F. Zhongwena, and L. Zhijun, "Energy Performance and Cost Comparison of MPPT Techniques for Photovoltaics and other Applications," *Energy Procedia*, vol. 107, pp. 297–303, 2017.

APPENDIX I

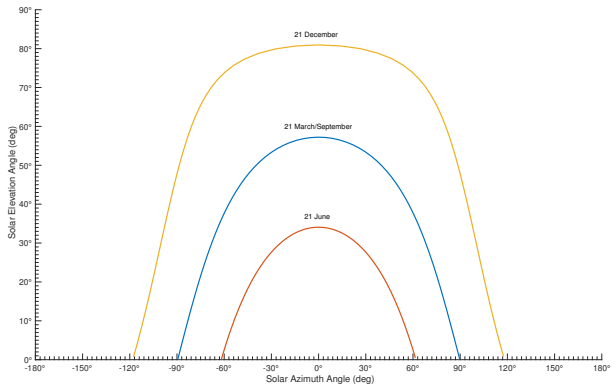

Fig. A1: Solar altitude at equinox and solstices

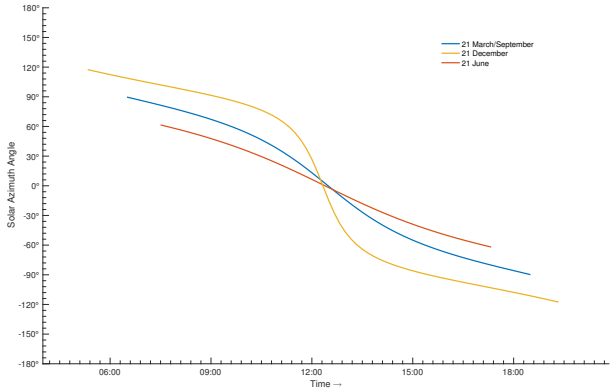

Fig. A2: Solar azimuth at equinoctes and solstices

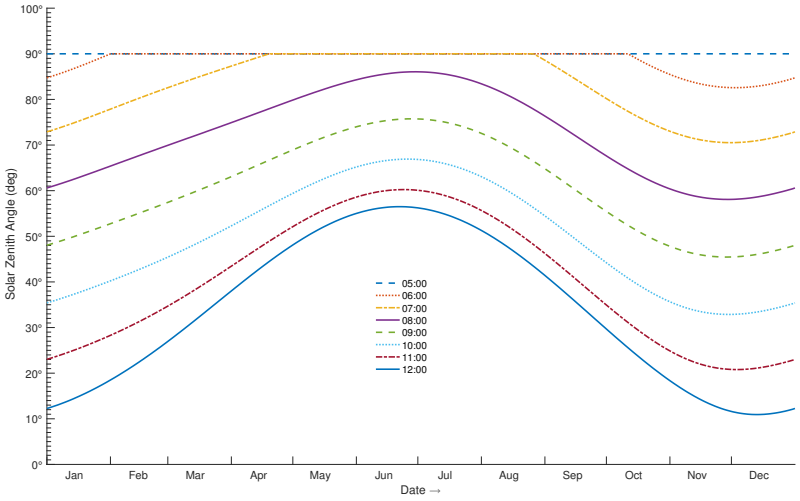

Fig. A3: Annual solar zenith angle at different times of day

Equation for weighting methodology:

$$\beta = \sum_{i=1}^{12} w_i \cdot \beta_i$$

$$\text{where } w_1 = \frac{I_1}{I_1 + I_2 + I_3 + ... + I_{12}}$$

($i =$ 1,2,...,12 are the months of the year)

TABLE III: Daily site insolation measurements and averages

	Total daily insolation	Peak insolation	Sun-hours
21 June	$2074.7\,\mathrm{kW\,h\,m^{-2}}$	$0.57\,\mathrm{kW\,m^{-2}}$	3.63 h
21 December	$5719.8\,\mathrm{kW\,h\,m^{-2}}$	$1.14\,\mathrm{kW\,m^{-2}}$	5.02 h
Average day	$3897.23\,\mathrm{kW\,h\,m^{-2}}$	$1.14\,\mathrm{kW\,m^{-2}}$	4.33 h

TABLE IV: Temperature measurements

Unoccluded summer noon	38.97 °C
Occluded summer noon	27.28 °C
Unoccluded winter noon	21.48 °C
Occluded winter noon	10.76 °C
Annual average	18.8 °C
Absolute maximum	40.3 °C
Absolute minimum	-3.95 °C
Absolute annual range	44.25 °C

TABLE V: Tilt Angles

	Angle	I_{total} [$\mathrm{kW\,h\,m^{-2}}$]
Weighted	28.92°	1440.88
Mean	33.95°	1439.76
Min	10.93°	1354.88
Max	56.49°	1300.59
Horizontal	0°	1236.84

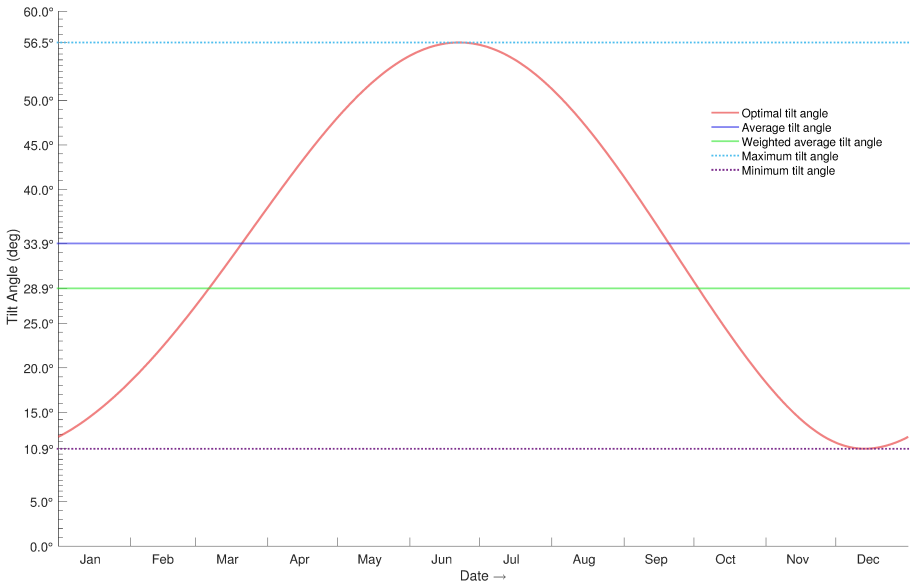

Fig. A4: Comparison of panel tilt angles

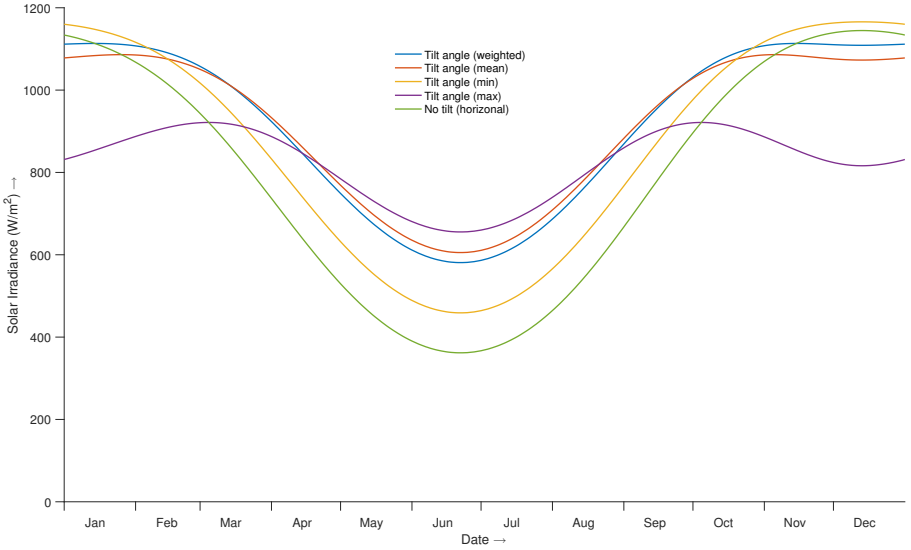

Fig. A5: The effect of tilt angle on insolation

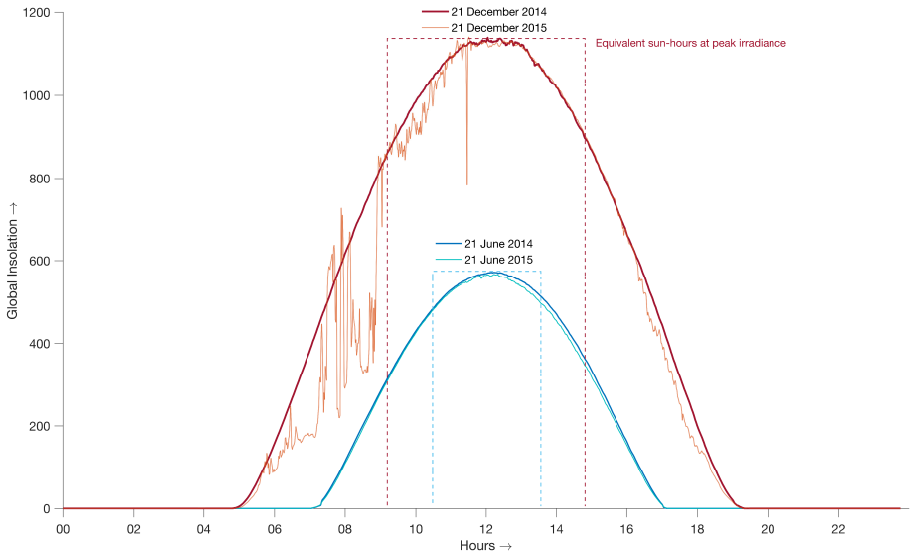

Fig. A6: Comparison of equinox insolation measurements

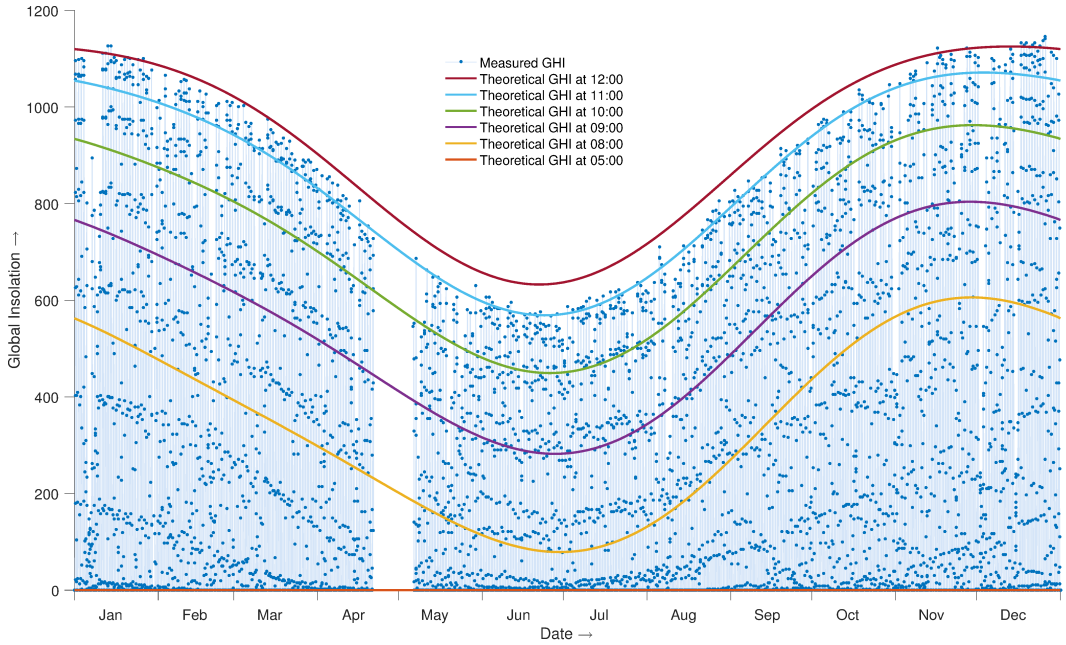

Fig. A7: Model of solar declination and zenith vs measured data

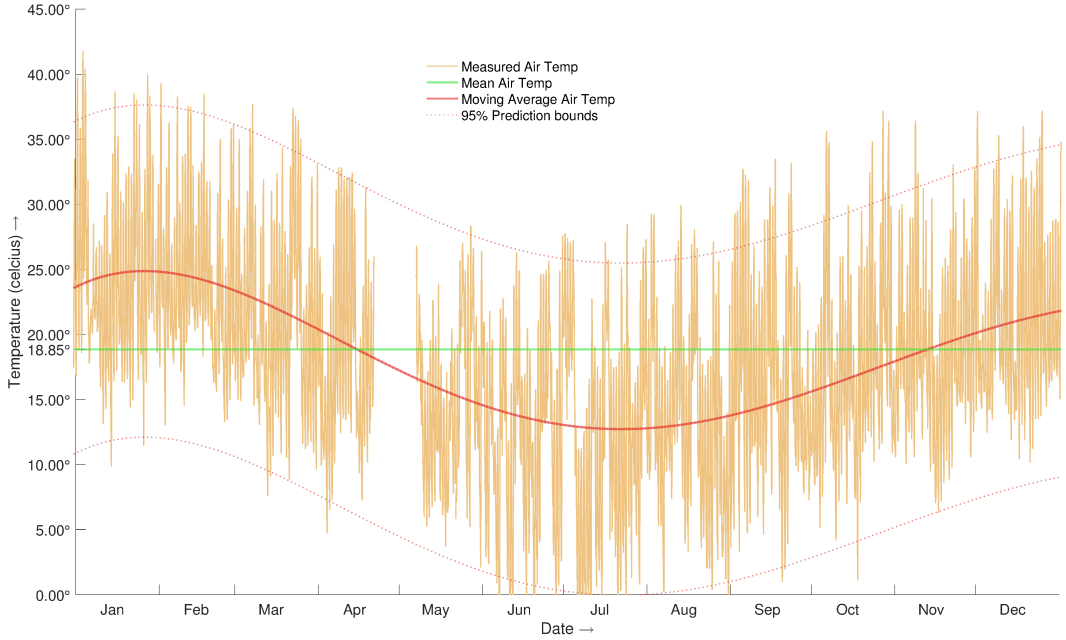

Fig. A8: Air temperature

Code 1: single_diode_model_calculations.m

```
I_ph = G_pu.*(I_sc_0 + alpha_I);
I_mpp = abs(G_pu.*(I_mp_0 + alpha_I));
V_oc = V_oc_0 - alpha_V;
V_mpp = V_mp_0 - alpha_V;
beta = G_pu.*(I_sc_0 + alpha_I);
gamma = 1/(V_mp_0 - V_oc_0) .* log((I_sc_0 - I_mp_0)./(I_sc_0 + alpha_I));
p = 1;

V = [0:0.5:50];
for i=1:numel(V)
    I(:,i) = G_pu.*(I_sc_0 + alpha_I) - beta.*exp(gamma.*(V(i) + alpha_V - V_oc_0));
    P(:,i) = V(i).*I(:,i);
    R(:,i) = V(i)./I(:,i);
end

[n m]  = size(P);
mpp_index =[];
for i=1:n
    [MPP(i) mpp_index(i)] = max(P(i,:));
    Load(i) = R(i,mpp_index(i));
end
```

TABLE VI: MPPT load simulation results

	Solar Peak [W m^{-2}]	Temp [°C]	I_{fixed} [A]	V_{fixed} [V]	R_{fixed} [Ω]	P_{fixed} [W]
Unoccluded summer noon	1139	38.97	4.31	43.1	10.0	185.76
Occluded summer noon	768	27.28	4.16	41.55	10.0	172.64
Unoccluded winter noon	571	21.48	3.86	38.6	10.0	149.00
Occluded winter noon	358	10.76	2.7	26.99	10.0	72.85

TABLE VII: Optimal load simulation results

	Solar Peak [W m^{-2}]	Temp [°C]	I_{mpp} [A]	V_{mpp} [V]	R_{mpp} [Ω]	P_{mpp} [W]
Unoccluded summer noon	1139	38.97	7.85	37.0	4.77	294.37
Occluded summer noon	768	27.28	5.73	27.0	4.77	156.71
Unoccluded winter noon	571	21.48	4.29	20.0	4.77	87.79
Occluded winter noon	358	10.76	2.70	13.0	4.77	34.91

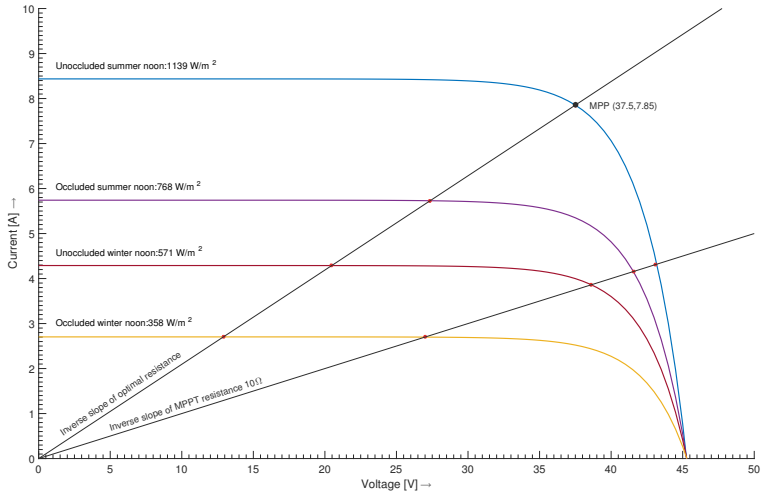

Fig. A9: Simulated IV curves, MPPs and intersection of line of fixed resistance

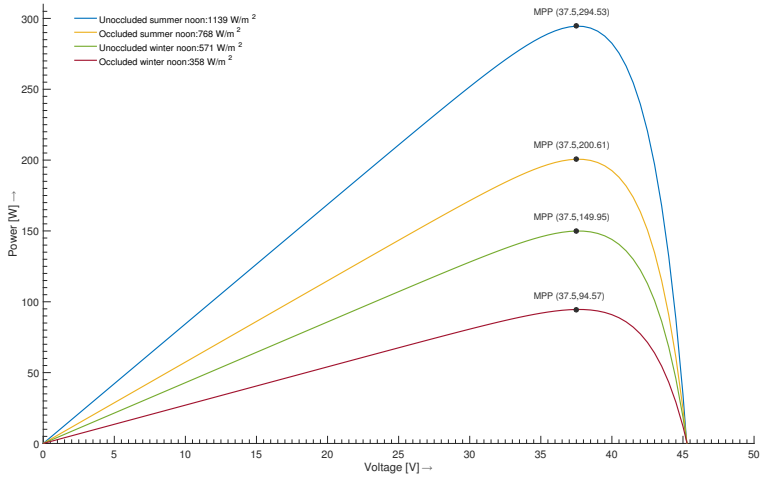

Fig. A10: Simulated PV curves

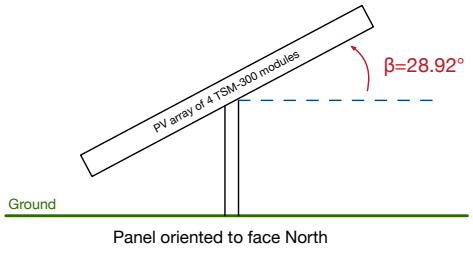

Fig. A11: Basic physical system

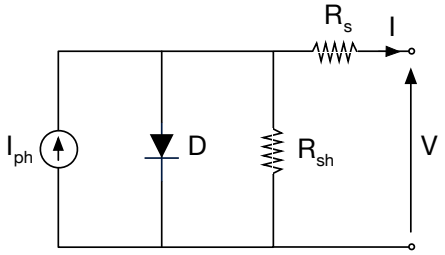

Fig. A12: Five parameter practical single diode model